Joint MEG-EEG signal decomposition using the coupled SECSI framework: Validation on a controlled experiment

Kristina Naskovska *, *Stephan Lau* §, *Amr Aboughazala* *, *Martin Haardt* *, and *Jens Haueisen* §
*Communications Research Laboratory, Ilmenau University of Technology, P. O. Box 100565, D-98684 Ilmenau, Germany
Email: kristina.naskovska, martin.haardt@tu-ilmenau.de
§Institute of Biomedical Engineering and Informatics, Ilmenau University of Technology, P. O. Box 100565, D-98684 Ilmenau, Germany

***Abstract*—Simultaneously recorded magnetoencephalography (MEG) and electroencephalography (EEG) signals can benefit from a joint analysis based on coupled Canonical Polyadic (CP) tensor decompositions. The coupled CP decomposition jointly decomposes tensors that have at least one factor matrix in common. The Coupled - Semi-Algebraic framework for approximate CP decomposition via SImultaneous matrix diagonalization framework (C-SECSI) efficiently estimates the factor matrices with adjustable complexity-accuracy trade-offs. Our objective is to decompose simultaneously recorded MEG and EEG signals above intact skull and above two conducting skull defects using C-SECSI in order to determine how such a tissue anomaly of the head is reflected in the tensor rank. The source of the MEG and EEG signals is a miniaturized electric dipole that is implanted into a rabbit's brain. The dipole is shifted along a line under the skull defects, and measurements are taken at regularly spaced points. The coupled SECSI analysis is conducted for MEG and EEG measurement series and ranks 1-3. This coupled decomposition produces meaningful components representing the three characteristic signal topographies for source positions under defect 1 and the positions on either side of defect 1. The rank estimation with respect to the complexity-accuracy trade-off of rank 3 reflects the three characteristic cases well and matches the dimensions spanned by the data set. The intact skull MEG signals show a higher complexity (rank 3) than the corresponding EEG signals (rank 1). The C-SECSI framework is a very promising method for blind signal separation in multidimensional data with coupled modalities, such as simultaneous MEG-EEG.**

I. Introduction

Tensor algebra preserves the structure of multidimensional signals. Therefore, it has applications in signal processing, data analysis, blind source separation and many more [1]. The multidimensional signals can be decomposed into rank one components according to the Canonical Polyadic (CP) decomposition [2]. In [3] a Semi-Algebraic framework for approximate CP decomposition via SImultaneous matrix diagonalization (SECSI) for the efficient computation of the CP decomposition is presented. Moreover, many combined signal processing applications can benefit from a coupled analysis based on the coupled CP decomposition [4], [5], [6].

The coupled CP decomposition jointly decomposes tensors that have at least one factor matrix in common. The computation of the coupled CP decomposition based on Alternating Least Squares (ALS) was analyzed in [7]. There it was shown that the computation of the coupled CP decomposition based on ALS is sensitive to different noise variances in the different tensors. The SECSI framework [3] was extended to the coupled SECSI (C-SECSI) framework in [8]. The C-SECSI framework efficiently approximates the coupled CP decomposition of two noisy tensors that have at least one mode in common even in ill-posed scenarios, e.g., if the columns of a factor matrix are highly correlated. Moreover, the C-SECSI framework offers adjustable complexity-accuracy trade-offs and efficiently decomposes tensors with different noise variances and without performance degradation. Furthermore, in [9] a reliability test for the C-SECSI framework was proposed. This reliability test allows us to control the rank of the coupled CP decomposition.

Electroencephalography (EEG) and magnetoencephalography (MEG) are clinical tools for diagnosing and locating pathologic brain function. They measure the electric potential (EEG) and the magnetic flux density (MEG) at the head surface that is generated by the electric currents of neuronal activity inside the brain. The head tissues act as a volume conductor that influences the measured signals. MEG and EEG signals can be measured simultaneously and complement each others information content. Therefore, a coupled analysis of MEG-EEG data using C-SECSI could be of great benefit. A conducting skull defect in the weakly conducting skull, e.g. after a surgery, is a volume conductor condition that can strongly influence MEG and EEG signals in characteristic ways [10], [11], [12], [13]. Therefore, MEG-EEG recordings above skull defects are a suitable case for validating signal decomposition algorithms.

In this study, our objective is to decompose simultaneously recorded MEG and EEG signals above intact skull and above two conducting skull defects in a controlled experimental setup using C-SECSI in order to determine how skull defects are reflected in the tensor decomposition.

II. Methods

A. Tensor Algebra and Notation

We use the following notation. Scalars are denoted either as capital or lower-case italic letters, A, a. Vectors and matrices are denoted as bold-face capital and lower-case letters, $\boldsymbol{a}, \boldsymbol{A}$, respectively. Tensors are represented by bold-face calligraphic letters $\boldsymbol{\mathcal{A}}$. The following superscripts, ^{T}, ^{H}, $^{-1}$, and $^+$ denote transposition, Hermitian transposition, matrix inversion and Moore-Penrose pseudo matrix inversion, respectively. The operators $||.||_{\mathrm{F}}$ and $||.||_{\mathrm{H}}$ denote the Frobenius norm and the higher order norm, respectively. Moreover, an n-mode product between a tensor $\boldsymbol{\mathcal{A}} \in \mathbb{C}^{I_1 \times I_2 \ldots \times I_N}$ and a matrix $\boldsymbol{B} \in \mathbb{C}^{J \times I_n}$ is defined as $\boldsymbol{\mathcal{A}} \times_n \boldsymbol{B}$, for $n = 1, 2, \ldots N$ [2]. A super-diagonal or identity N-way tensor of dimensions $R \times R \ldots \times R$ is denoted as $\boldsymbol{\mathcal{I}}_{N,R}$. The n-th 3-mode slice of $\boldsymbol{\mathcal{A}} \in \mathbb{C}^{I \times J \times N}$ is denoted as $\boldsymbol{\mathcal{A}}_{(.,.,n)}$ and accordingly one element is denoted as $\boldsymbol{\mathcal{A}}_{(i,j,n)}$.

The CP tensor decomposition of a tensor $\boldsymbol{\mathcal{X}} \in \mathbb{C}^{M_1 \times M_2 \times M_3}$ with rank R can be written as

$$\boldsymbol{\mathcal{X}} = \boldsymbol{\mathcal{I}}_{3,R} \times_1 \boldsymbol{F}_1 \times_2 \boldsymbol{F}_2 \times_3 \boldsymbol{F}_3,$$

where $\boldsymbol{F}_1 \in \mathbb{C}^{M_1 \times R}$, $\boldsymbol{F}_2 \in \mathbb{C}^{M_2 \times R}$, and $\boldsymbol{F}_3 \in \mathbb{C}^{M_3 \times R}$ are the factor matrices. If two tensor $\boldsymbol{\mathcal{X}}^{(1)} \in \mathbb{C}^{M_1^{(1)} \times M_2 \times M_3^{(1)}}$ and $\boldsymbol{\mathcal{X}}^{(2)} \in \mathbb{C}^{M_1^{(2)} \times M_2 \times M_3^{(2)}}$ have the second mode in common, than they have a coupled CP decomposition.

$$\boldsymbol{\mathcal{X}}^{(1)} = \boldsymbol{\mathcal{I}}_{3,R} \times_1 \boldsymbol{F}_1^{(1)} \times_2 \boldsymbol{F}_2 \times_3 \boldsymbol{F}_3^{(1)}$$
$$\boldsymbol{\mathcal{X}}^{(2)} = \boldsymbol{\mathcal{I}}_{3,R} \times_1 \boldsymbol{F}_1^{(2)} \times_2 \boldsymbol{F}_2 \times_3 \boldsymbol{F}_3^{(2)}$$

For the mode in common, i.e., mode two, both tensors have the same factor matrix. The C-SECSI framework approximates the coupled CP decompositions using the tensor structure to construct not only one but the full set of possible Simulations Matrix Diagonalizations (SMDs) jointly for both tensors [8]. By solving all SMDs, multiple estimates of the factor matrices are obtained. As explained in [8] and [9], some

978-1-5386-1251-4/17/$31.00 ©2017 IEEE

of these estimates are obtained jointly and some of the estimates are obtained separately. Using for instance the heuristic REConstructed Paired Solutions (REC PS) the final solution is chosen based on the reconstruction error [3]. The reconstruction error is calculated according to

$$e_{\mathrm{rec}} = \frac{\left|\left|\hat{\boldsymbol{\mathcal{X}}} - \boldsymbol{\mathcal{X}}\right|\right|_{\mathrm{H}}^2}{||\boldsymbol{\mathcal{X}}||_{\mathrm{H}}^2}. \tag{1}$$

Moreover, in [9] a reliability error,

$$e_{\mathrm{r}} = \frac{\left|\left|\hat{\boldsymbol{F}}_2^{(2)} - \hat{\boldsymbol{F}}_2^{(1)}\right|\right|_{\mathrm{F}}^2}{\left|\left|\hat{\boldsymbol{F}}_2^{(1)}\right|\right|_{\mathrm{F}}^2}, \tag{2}$$

was defined as a measure of the error between the final estimate of the common factor matrices. This reliability error has a minimum if the final estimates result from the coupled solution and the assumed low rank is correctly approximated. Therefore, the reliability error can be used to control the tensor rank of the coupled approximate CP decompositions. Therefore, it can provide a rank estimate of the coupled low rank tensors. Note that for tensor rank one the reliability error is always zero within the machine accuracy. This is due to the fact that for rank one tensors the C-SECSI framework does not calculate any SMD. In this case, the final estimate of the factor matrices is provided from the joint truncated High Order Singular Value Decomposition (HOSVD). In general, the factor matrices of the CP and the coupled CP decomposition can be identified up to scaling and permutation ambiguity.

B. Measured MEG-EEG Signals

In a previous study [12], a miniaturized electric dipole was implanted in vivo into a rabbit's brain and connected to a 20 Hz sinusoidal constant-current source. Simultaneous recording using 64-channel EEG and 16-channel MEG was conducted, first without defect (WOD) and then with two skull defects (WD). Skull defects were filled with agar gels, which had been formulated to have a time-stable conductivity of approx. 1.0 S/m. The dipole was moved under the skull defects, and measurements were taken at regularly spaced points. The signals were sampled at 1 kHz, band-pass filtered (15-25 Hz) and approx. 300 consecutive trials each were averaged. All MEG and EEG recordings, respectively, were co-registered and resampled to a common set of virtual channels. We combined the measurements in two tensors $\boldsymbol{\mathcal{T}}_{\mathrm{MEG}}$ and $\boldsymbol{\mathcal{T}}_{\mathrm{EEG}}$ with the four dimensions: channel $\times$ time point $\times$ defect state (WOD = 1, WD = 2) $\times$ dipole position.

C. MEG-EEG Signal Decomposition

In a subsequent step we have constructed the following tensors:

$$\boldsymbol{\mathcal{T}}_{\mathrm{MEG,WOD}} = \boldsymbol{\mathcal{T}}_{\mathrm{MEG}(.,.,1,.)} \quad \boldsymbol{\mathcal{T}}_{\mathrm{EEG,WOD}} = \boldsymbol{\mathcal{T}}_{\mathrm{EEG}(.,.,1,.)}$$
$$\boldsymbol{\mathcal{T}}_{\mathrm{MEG,WD}} = \boldsymbol{\mathcal{T}}_{\mathrm{MEG}(.,.,2,.)} \quad \boldsymbol{\mathcal{T}}_{\mathrm{EEG,WD}} = \boldsymbol{\mathcal{T}}_{\mathrm{EEG}(.,.,2,.)}$$

All of the tensors are normalized to norm one tensors, for instance $\boldsymbol{\mathcal{T}}_{\mathrm{EEG,WOD}} = \boldsymbol{\mathcal{T}}_{\mathrm{EEG,WOD}} / ||\boldsymbol{\mathcal{T}}_{\mathrm{EEG,WOD}}||_{\mathrm{H}}$. The indexes MEG and EEG represent the MEG and EEG signal tensors, respectively. The tensors $\boldsymbol{\mathcal{T}}_{\mathrm{EEG,WOD}}$, $\boldsymbol{\mathcal{T}}_{\mathrm{EEG,WD}}$, represent the EEG signal tensors for all available positions, without skull defect (WOD) and with skull defect (WD), respectively. Accordingly, the tensors $\boldsymbol{\mathcal{T}}_{\mathrm{MEG,WOD}}$, $\boldsymbol{\mathcal{T}}_{\mathrm{MEG,WD}}$, represent the MEG signal tensor without and with skull defect, respectively, for all available positions. Therefore, the tensors have the dimensions channel $\times$ time point $\times$ dipole position.

For all of the above defined tensors, the coupled CP decomposition based on the C-SECSI framework is computed for different tensor ranks, $R = 1, 2, 3$. The coupled CP decomposition is computed for the two pairs of MEG-EEG signal tensors by assuming that time is the common mode.

III. Results

A. Rank and Reconstruction Error

The reconstruction errors for each of the MEG and EEG signal estimates using the C-SECSI framework are depicted in Table I. This reconstruction error decreases as the assumed rank increases. Moreover, in Table I the reliability error for each of the coupled CP decompositions is depicted. Based on these errors, the MEG and EEG signals with defects have one identical component in the time mode and one of them has additional components. The MEG and the EEG signal tensors without defects share one component in the time mode. Considering all of the results, more components can be extracted for the MEG signal with skull defect then for the rest of the signals.

	R = 1	R = 2	R = 3
Reconstruction error for the MEG signal tensors			
MEG WD	0.029	0.007	0.001
MEG WOD	0.128	$8.5 \cdot 10^{-4}$	$3.1 \cdot 10^{-9}$
Reconstruction error for the EEG signal tensors			
EEG WD	0.065	0.0034	$6.9 \cdot 10^{-4}$
EEG WOD	0.335	0.004	0.013
Reliability error for the coupled CP decomposition			
WD (EEG-MEG)	$1.9 \cdot 10^{-32}$	$1.1 \cdot 10^{-5}$	$5.4 \cdot 10^{-5}$
WOD (EEG-MEG)	0	0.15	0.194

TABLE I: Reconstruction error for the MEG and EEG signal tensors and reliability error for the coupled CP decomposition.

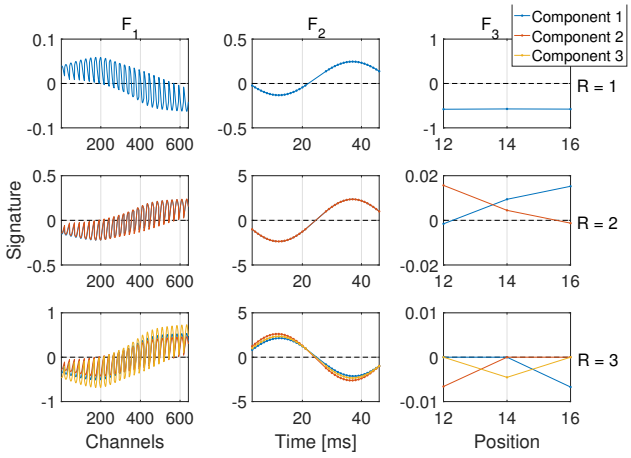

Fig. 1: Components of the MEG signal tensor without skull defect resulting from the coupled EEG-MEG, CP decomposition for tensor rank $R = 1, 2, 3$ (first, second, and third row, respectively). The curves in blue, red, and yellow represent component 1, component 2, and component 3, respectively.

To present our results, we depict some of the factor matrices resulting from the tensor decompositions. In Fig. 1 we illustrate the components of the MEG signal without skull defect as a result of the coupled EEG-MEG signal decomposition for tensor rank $R = 1, 2, 3$. By analyzing the signature of the positions in this figure we can see that for $R = 3$ each of the components is related to one of the positions, i.e., position 12, positions 14, and position 16. The components of the MEG signal with skull defect as a result of the coupled EEG-MEG signal decomposition for tensor rank $R = 1, 2, 3$

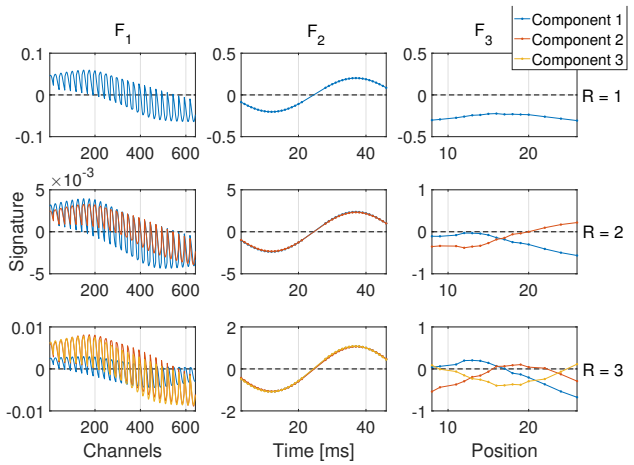

Fig. 2: Components of the MEG signal tensor with skull defect resulting from the coupled EEG-MEG, CP decomposition for tensor rank $R = 1, 2, 3$ (first, second, and third row, respectively). The curves in blue, red, and yellow represent component 1, component 2, and component 3, respectively.

are depicted in Fig. 2. Based on the signature of the dipole position it is noticeable that the changes in the signature of the channels correspond to the position changes. Therefore, for the MEG signal tensors with defect, more signal components can be extracted, as it was expected based on the reconstruction and reliability error.

B. MEG Signal Components

Fig. 3 shows the rank 3 components computed based on the coupled decomposition of the MEG signals above the two skull defects. The measured MEG signals (top row) of the tangential source experience changes in position, orientation, and amplitude [12]. Component 2 (second row) of the tensor decomposition reflects primarily the MEG signals at the lowest source positions. Component 3 (third row) models the mid-range of source positions. The highest source positions are represented by a combination of component 1 (row 4) and component 2. The gradual transition of component amplitudes is also reflected in the lower right diagram of Fig. 2. The rank 2 decomposition in row 2 of Fig. 2 (field-maps omitted due to space constraints) models the measurements with one or two components, but the difference in source position is not as well differentiated as with rank 3. With rank 1 (field-maps omitted), the one component represents the mid-range source positions best with errors increasing towards low and high source positions.

Without skull defects, the coupled decomposition is based on three available measurements (pos. 12, 14, and 16). Therefore, the rank 3 result trivially represents each measurement with one component, which can be seen in the lower right diagram of Fig. 1 (field-maps omitted). Assuming rank 2, the two components represent primarily the lowest and highest source position, respectively, whereas position 14 is represented by both components (see Fig. 1, field-maps omitted). Using rank 1, the single component represents the middle source position best with errors increasing towards low and high positions.

C. EEG Signal Components

Fig. 4 shows the components from the rank 3 coupled decomposition of the EEG signals above the two skull defects. The measured EEG signals (top row) of the tangential source experience a reversal of polarity above defect 1 depending on which pole is closer to it [12]. When the source is approximately central under the defect 1, the overall topography is bipolar, but with distortions above that skull defect. Component 3 represents the defect-related monopolar signal at the lowest positions of both defects. Component 1 represents the source positions close to the center of the defect and bipolar aspects related to defect 2. Component 2 captures the monopolar signal increase above defect 1 at middle and high positions. The strength of the components transitions across the position range.

Without skull defects, a rank 3 coupled decomposition represents the measured EEG signals primarily with one component only (field-maps omitted). This matches the fact that the three source positions only span 0.7 mm along the shift axis and, therefore, are very similar if the skull is intact. However, the decomposition separated the common signal from an instance of noise in the measurement at position 12. Assuming rank 2 or rank 1, the minor components are eliminated stepwise.

IV. Discussion

The decomposition of the measured MEG and EEG signals using C-SECSI produces meaningful components with respect to the experimental setup. The main dimension to be decomposed is the source position, along which the signal changes due to the skull defects appear. Based on the experimental results [12], the range of source positions can be broadly divided into three cases, the positions under defect 1 and the positions on either side of defect 1. This is reflected in the three components of the rank 3 decomposition of MEG and EEG signals, respectively. The gradual transition between the cases along the source position series is modeled by the combination of two components. The defect-related EEG signals are up 10 times as strong as the intact skull EEG signals, whereas the amplitude difference in the MEG signals is only approx. 24 % [12]. Consequently, the components of the EEG signals reflect mostly defect-related aspects and the MEG signal components reflect changes in source position jointly with the defect-related changes.

The measurements without defects show a difference in rank between MEG and EEG signals. The EEG measurements are primarily represented by one component only (rank 1), whereas the simultaneously measured MEG signals are estimated with three components (rank 3). This may be due to the stronger topographic difference of the MEG signals between source positions as well as the higher topographic complexity in this experimental setup.

The experimental setup with skull defects involves even more than three conceptual components. For example, defect 1 and defect 2 may be differentiated and the intact skull signal component could be isolated in the defect measurements. However, the available data samples do not span these dimensions with sufficiently many data points. Consequently, the rank estimation and decomposition identify only the three components in the data.

V. Conclusion

Using the C-SECSI framework, coupled MEG-EEG signals above intact skull and above two conducting skull defects were decomposed in order to determine the influence of the skull defects in the tensor decomposition. Meaningful components were successfully extracted representing the three characteristic signal topographies for the source position. The C-SECSI framework is a very promising method for blind source separation, signal decomposition within the source reconstruction workflow, and for signal artifact extraction. The multimodal integration of MEG and EEG signals through their coupling can improve the localisation accuracy in clinical diagnostics, pre-surgical planning, and functional mapping of the human brain.

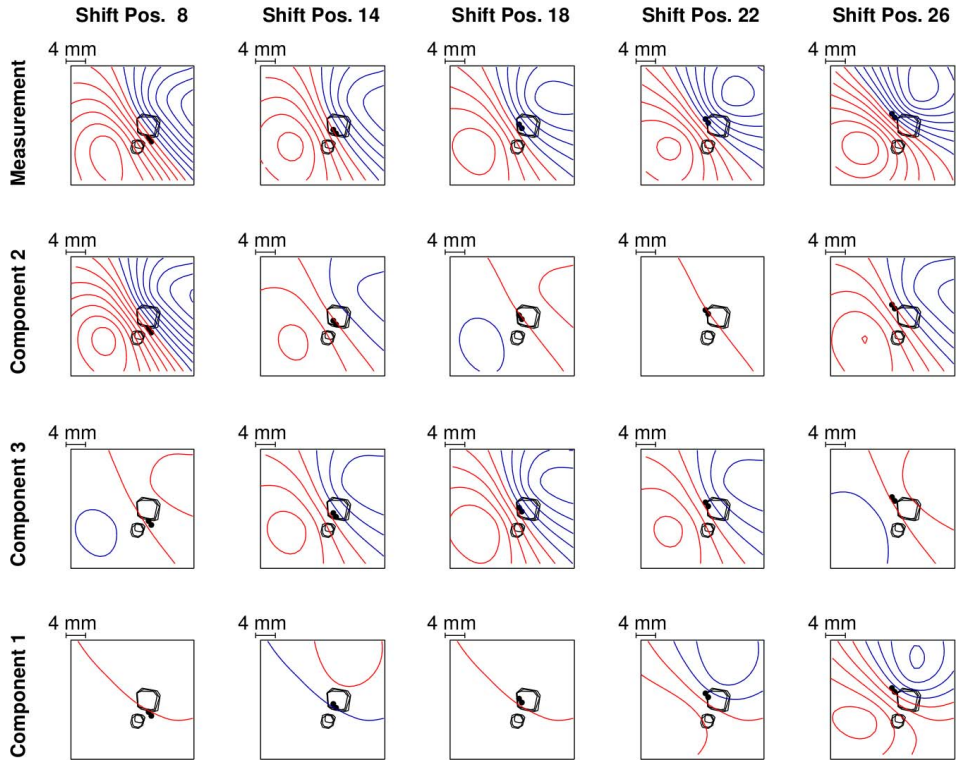

Fig. 3: Measured MEG signals above two skull defects (row 1) and components of rank 3 coupled decomposition (rows 2-4) shown at selected source positions (columns) at the first peak in the time dimension. The iso-line increment is uniform within measurements and within components, respectively. The components are arranged in a meaningful sequence. The dipolar source is indicated with a black bar with two spheres marking the poles. Skull defects are marked by closed black lines indicating the inner, middle and outer boundaries of the defects.

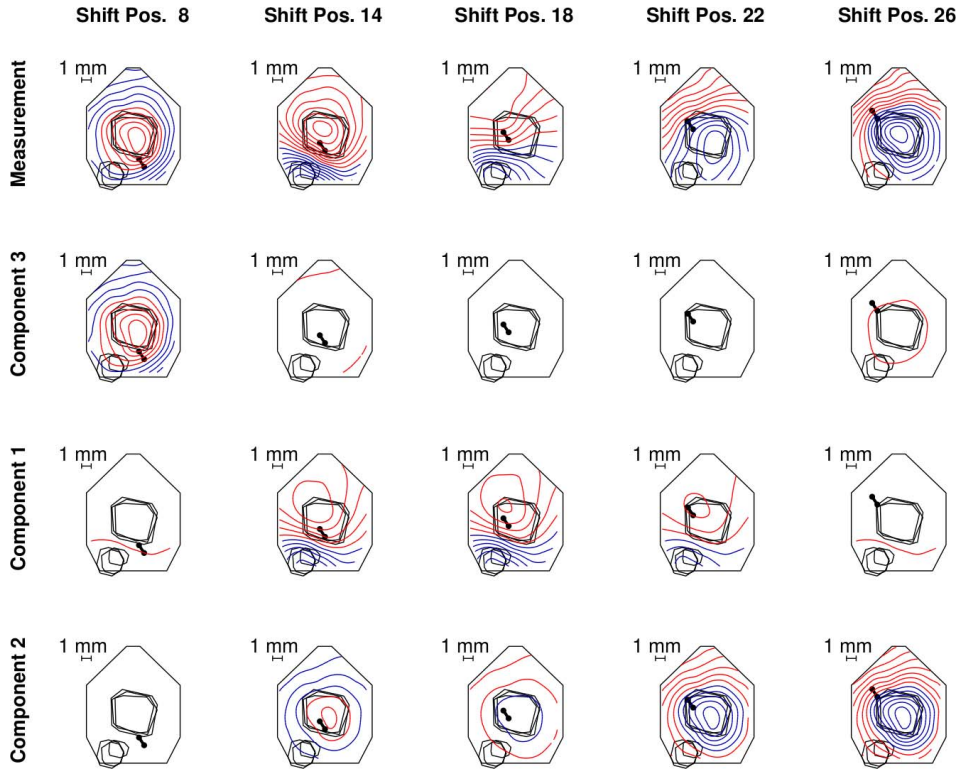

Fig. 4: Measured EEG signals above two skull defects (row 1) and components of rank 3 coupled decomposition (rows 2-4) shown at selected source positions (columns) at the first peak in the time dimension. Formatting and markings equivalent to Fig. 3.

REFERENCES

[1] A. Cichocki, D. Mandic, A. Phan, C. Caiafa, G. Zhou, Q. Zhao, and L. de Lathauwer, "Tensor decompositions for signal processing applications: From two-way to multiway," *IEEE Signal Processing Magazine*, vol. 32, pp. 145–163, 2015.

[2] T. Kolda and B. Bader, "Tensor decompositions and applications," *SIAM Review*, vol. 51, pp. 455–500, 2009.

[3] F. Roemer and M. Haardt, "A semi-algebraic framework for approximate CP decomposition via simultaneous matrix diagonalization (SECSI)," *Signal Processing*, vol. 93, pp. 2722–2738, September 2013.

[4] E. Acar, R. Bro, and A. K. Smidle, "Data fusion in metabolomics using coupled matrix and tensor factorization," *Proceedings of IEEE*, vol. 103, pp. 1602 – 1620, August 2015.

[5] E. Acar, T. G. Kolda, and D. M. Dunlavy, "All-at-once optimization for coupled matrix and tensor factorizations," *MLG11: Proceedings of Mining and Learning with Graphs*, August 2011.

[6] H. Becker, P. Comon, and L. Albera, "Tensor-based preprocessing of combined EEG/MEG data," *in Proc. 20-th European Signal Processing Conference (EUSIPCO 2012), Bucharest, Romania*, Oct. 2012.

[7] J. Cohen, R. Farias, and P. Comon, "Joint tensor compression for coupled canonical polyadic decompositions," *in Proc. 24th European Signal Processing Conference (EUSIPCO 2016)*, August 2016.

[8] K. Naskovska and M. Haardt, "Extension of the semi-algebraic framework for approximate CP decompositions via simultaneous matrix diagonalization to the efficient calculation of coupled CP decompositions," *in Proc. of 50th Asilomar Conf. on Signals, Systems, and Computers*, Nov. 2016.

[9] K. Naskovska, A. A. Korobkov, M. Haardt, and J. Haueisen, "Analysis of the photic driving effect via joint EEG and MEG data processing based on the coupled CP decomposition," *in Proc. 25-th European Signal Processing Conference (EUSIPCO 2017), Kos Island, Greece*, Sept. 2017.

[10] W. Cobb, R. Guiloff, and J. Cast, "Breach rhythm. the EEG related to skull defects," *Electroencephalography and Clinical Neurophysiology*, vol. 47, pp. 251–271, 1979.

[11] J. Lee, N. Tanaka, H. Shiraishi, T. Milligan, B. Dworetzky, S. Khoshbin, S. Stufflebeam, and E. Bromfield, "Evaluation of postoperative sharp waveforms through EEG and magnetoencephalography," *Journal of Clinical Neurophysiology*, vol. 27, pp. 7–11, 2010.

[12] S. Lau, L. Flemming, and J. Haueisen, "Magnetoencephalography signals are influenced by skull defects," *Clinical Neurophysiology*, vol. 125, pp. 1653 – 1662, 2014.

[13] S. Lau, D. Guellmar, L. Flemming, D. B. Grayden, M. J. Cook, C. H. Wolters, and J. Haueisen, "Skull defects in finite element head models for source reconstruction from magnetoencephalography signals," *Frontiers in Neuroscience*, vol. 10, article 141, 2016.